A study on soil loss rate assessment of vegetation mat measures

Han, Eun Jin; Park, Yong Sung; Kim, Young Do; Park, Jae Hyeon

Published in:
Journal of Hydro-environment Research

DOI:
10.1016/j.jher.2015.10.001

Publication date:
2016

Document Version
Peer reviewed version

A Study on Soil Loss Rate Assessment of Vegetation Mat Measures

Eun Jin Han[1], Yong Sung Park[2], Young Do Kim[1*], Jae Hyeon Park[3]

[1]Department of Environment Engineering, Inje University, 197 Inje-ro, Gimhae, Gyeongnam 50834, Republic of Korea
[2]Division of Civil Engineering, University of Dundee, Nethergate, Dundee, DD1 4HN, Scotland, UK
[3]Department of Civil Engineering, Inje University, 197 Inje-ro, Gimhae, Gyeongnam 50834, Republic of Korea

Abstract: *The hydraulic stability of the high-water revetment with and without vegetation mat was tested in both laboratory-scale hydraulic experiments, as well as prototype-scale experiments. Experimental cases cover a wide range of cross-sectional average velocity (0.2 to 2.0 m/s), different slopes of the embankment, and two different types of soils. For each experimental condition, measurements of velocity field and scouring profile on the embankment were repeated for the cases with and without vegetation mat, respectively, to assess the efficiency of the vegetation mat in protecting the embankment. A dramatic reduction in soil loss rate was observed in the cases with the vegetation mat installed. The experimental results were recast in terms of Froude number and the soil loss rate appears to be proportional to the square of Froude number. Also a functional relationship between the soil loss rate and the cross-sectional average velocity was also deduced so that it could guide actual design practices of such high-water revetments. To the authors' best knowledge, the current study is the first to attempt to provide a practical design guideline.*

Keywords: *High-water revetment, Hydraulic stability, Prototype experiment, Vegetation mat.*

1. Introduction

In many riverine or coastal areas, various revetment techniques can be applied simultaneously to maximize the efficiency and usability of the structure. For example, the lower part of the revetment, which would be in constant contact with flowing water, may be fitted with rigid soil, while the upper part can be covered with soft soil that is more suitable for vegetation. Despite the potential effectiveness of such practice, however, there has not been any systematic study of the selection criteria and the revetment design technique, which has hindered practical application of the technique. Since the late 1990s in Korea, recognition of the importance of the riverine environment has been increasing, but without adequate selection criteria or design standards, revetment techniques using vegetation mats have been often determined by subjective judgments and particularly by a simple estimate of the tractive force without considering hydraulic characteristics (Busan Regional Construction Management Administration, 2008).

Of course, the above-mentioned current practice may not be entirely unjustified. Vegetative linings can fail with increased shear stress, either by particle detachment or failure of the individual vegetal elements. Also, there have been a considerable number of studies performed in developing resistance laws for channels with flexible vegetation (Kouwen and Unny, 1973; Temple et al., 1987; Kouwen and Fathi-Moghadam, 2000; Järvela, 2004). Recently, furthermore, several studies have focused on the velocity profiles and the turbulent characteristics of vegetated channels (Shimizu and Tsujimoto, 1994; Naot et al., 1996; Nepf, 1999; Lápez and Garcıa, 2001; Stephan and Gutknecht, 2002). However, systematic research on the hydraulic characteristics and the patterns of soil erosion depending on the vegetation mat of a high water revetment is still lacking.

To reiterate, while a vegetation mat is often used in river bank naturalization projects, its hydraulic characteristics and stability have not been thoroughly studied. In particular, to the authors' knowledge, no study has focused on the rate of soil loss, despite its obvious importance in the hydraulic stability of river banks. Therefore, to fill this knowledge gap, this study aims to investigate the hydraulic safety of

revetment through laboratory-scale and prototype experiments. We measured the rate of soil loss for cases with and without a vegetation mat, thereby evaluating the stability of the vegetation mat method. These experimental results of the relative soil loss rate can be used for evaluating the relationship between the cross-sectional velocity and the soil loss rate at the high-water revetment.

We present some theoretical considerations in the next section. The experimental setup and cases are discussed in section 3. In section 4, the experimental results are presented and discussed. Finally, concluding remarks are presented in section 5.

2. Theoretical considerations

In this study, we are interested in the rate of soil loss in rivers. Naturally, the soil loss rate should be dependent on geometric and hydraulic properties of the channel, flow rate and also the mechanical properties of soils. As explained in the next section, in which the experimental setup and cases are discussed, however, it is technically challenging to vary soil properties over a wide range, especially with the need to grow vegetation on each soil for a long time. As a result, there are only two different soil types used in the experiments: one is excavated from a natural river and the other is prepared in the laboratory with which we grew vegetation (see Section 3 for more information). On the other hand, we were able to create a wide range of conditions for the other factors.

For erosion processes on riverbed, an important hydraulic property of the flow is bed shear stress, τ. In the sense of reach-averaged value, bed shear stress only depends on the geometric properties of the channel by the following formula:

$$\tau = \gamma RS, \qquad \text{(Eq. 1)}$$

in which γ is the specific gravity of water, R is the hydraulic radius, and S is the energy slope of the channel. On the other hand, the flow rate Q is also determined by R and S, as dictated by Manning's formula (for SI unit):

$$Q = \frac{1}{n} R^{2/3} S^{1/2}, \qquad \text{(Eq. 2)}$$

in which, n is Manning's roughness coefficient. Now considering Equations (1 & 2), it seems natural to introduce a Froude number based on the flow rate and hydraulic radius, namely

$$Fr_R = \frac{Q}{A\sqrt{gR}}, \qquad \text{(Eq. 3)}$$

in which A is the cross-sectional area, and g is the gravitational acceleration. We reiterate here that Fr_R reflects both hydraulic (i.e. flow rate and bed shear stress) and geometric properties of the flow in the channel.

Alternatively, we also introduce a Froude number based on the nominal water depth, h, as below:

$$Fr_h = \frac{Q}{A\sqrt{gh}}. \qquad \text{(Eq. 4)}$$

Considering that the hydraulic radius is half the radius of a circular cross-section with the same cross-sectional area of the channel, we define our nominal water depth as the depth of a channel with a rectangular cross-section with the same cross-sectional area, i.e.

$$h = \frac{A}{w}, \qquad \text{(Eq.6)}$$

where w is the width of the channel at the free surface. Note that the nominal depth h is always greater

than the hydraulic radius R, therefore Fr_h is always less than Fr_R. However the difference becomes negligible in a wide channel, as R asymptotically approaches h.

3. Experimental setup and cases

3.1 Laboratory-scale experiments

In this study, laboratory-scale experiments were conducted in a 14-m-long and 1.2-m-wide re-circulating grass-wall flume. Experimental cases are listed in tables 1 and 2, where u is the cross-sectional average velocity.

Table 1. Experimental cases and results (Series SV)

Table 2. Experimental cases and results (Series HV)

Fig. 1 shows the schematic diagram of the experimental flume with the measuring devices. As shown in Fig.1, on the left side of the channel (viewed towards upstream) is a sloping embankment made of acrylic. There are two 1.2-m-long stations in the embankment, where soil and vegetation are mounted for experiments. To reduce the flow cross-section and thereby to increase the flow velocity, a vertical wall is installed on the right side of the channel. A photograph of the experimental channel with the acrylic embankment and the vegetation installed is in Fig. 2.

Fig. 1. Schematic diagram of the experimental channel.

Fig. 2. Acrylic embankment and vegetation mat installed in the channel

We used two different kinds of vegetation mats. For the series SV, we excavated a part of vegetated embankment from a natural river, which consists of fine silt with d_{50} = 0.08 mm. We also grew vegetation indoors for four weeks in a sandy soil with d_{50} = 0.46 mm. Note that this is the same kind of soil that is used in actual practice of such revetment techniques. When the grass became 10 cm tall, we replanted them n the sloped embankment while protecting the roots of the vegetation, which then was used for the series HV (for the experimental cases, see tables 1 and 2). Fig. 3 shows the excavated natural vegetation as well as the vegetation mat we grew indoors. Also photographs taken at two different growth stages of the vegetation mat are presented in Fig. 4. We note here that, due to substantial time and effort required to prepare for vegetation mats, we could not repeat the experiments with a wide range of soil properties. By comparing the results from the two series, however, we intend to see general effects of soil conditions on the soil loss rate.

Fig. 3 Vegetation and vegetation mat installed in the channel

Fig. 4 Vegetation mat growing processes (after 2weeks and 4weeks, respectively)

In this study, the soil loss rates for the various hydraulic conditions and the vegetation conditions are examined via hydraulic experiments. The flow velocities and the water depths were measured to calculate the flowrates and the Froude Numbers. The scouring depths were also measured to calculate the soil loss rate. The time averaged spatial velocity distribution was measured using a Micro-ADV (Nortek Vectrino, N-7781) 3-Dimensional velocity meter. The scouring depth of the sediment layer for relative soil-loss rate was measured using a sand surface meter (KENEK, WHT-60) both before and after each experimental

run at three location within the sediment layer, that is at the center and 10 cm away from the center in both upstream and downstream direction. At each location, scour depths were measured at a spacing of 2 cm in the lateral direction, and the results from the three locations in the streamwise direction were averaged to estimate the soil loss rate.

For the experimental cases with the artificially grown vegetation mats, the slope of the embankment was measured before the vegetation mats were installed. Experiments were carried out only after the roots of the vegetation firmly attached to the embankment and scour depths were measured after carefully removing the vegetation mats. To avoid any disturbance in the soil embankment while removing the vegetation mats, roots were carefully cut before scour depth measurements.

Before embarking on the experimental campaign, we carried out a few test runs to make sure that the soil loss rate measurement is more or less repeatable for the same hydraulic conditions and soil conditions. For the main experiments, however, only one experiment was performed for each case. This is because growing the vegetation mats and attaching them onto the embankment take considerably long time, and we had to choose between repeating the same cases and increasing the number of experimental cases. After completing measurements for each case, we replaced the used wet soil with dry soil, on which the vegetation mat was attached, so that each case in each series starts with identical moisture content and cohesiveness.

The time required for scour depth to reach equilibrium state in clear-water scouring condition was estimated from the test runs, and based on this result, each of main experiments continued for 20 minutes before measuring scour depth.

3.2 Prototype-scale experiments

The prototype-scale experiments were conducted in a 500-m-long by 10-m-wide re-circulating grass-wall flume in the multi-functional river experiment station in Korea (Fig. 5). Experimental cases are listed in table 3.

Table 3. Experimental cases and results (Series PV)

The multi-functional river experiment station is organized with three test waterways, three test lakes, an inflow water tank and water storage, an inflow pump, lighting and monitoring facilities, and a test laboratory. The A1 waterway was installed for a scale test, including revetment stability, and for securing 5 m/s of the maximum flow velocity. The A2 waterway is used to test an interrelationship between the physical structure and the ecological structure through long-term ecological monitoring. Finally, the A3 waterway is used for an experiment on the hydraulic characteristics of the river structures and vegetation.

Fig. 6 shows the vegetation mats used in the prototype-scale experiments. Note that the same vegetation and soil as in the series HV were used. The experiments were performed in A1 waterway, and the soil loss rate was analyzed by observing the changes in the bed elevations. Additionally, the flow velocities were measured to calculate the flow rate and the relevant quantities.

Fig. 5. Multi-functional river experiment station in Korea

Fig. 6. Vegetation mats installed in the experimental channel

The experimental work in this study concentrated on determining the hydraulic capacity of the grassed revetment. During the experiments, measurements were taken of the water depth, the soil loss rate and flow velocities at the measuring sections. It was observed that the more the flow rate increases, the more the velocity increases as well. The sand surface meter was used to estimate the soil loss rate, and the velocity was measured using an ADV (Sontek-FlowTracker).

4. Results and discussion

4.1 Laboratory-scale experiments

Table 1 summarizes the SV test results. Overall, cases with vegetation exhibit 2 to 11% less soil loss, demonstrating the protective effect of vegetation. In particular, the average soil loss rate in the cases without a vegetation mat (SV 1 to 9) was 7.85%, and that of the cases with a vegetation mat (SV 10 to 18) was 2.83%. Among the experimental cases, the greatest soil loss rate was observed for the case with the slope 1:2.0.

As an example, Fig. 7 presents the experimental results for the cases SV 6 and SV 15. The figure shows cross-sectional view of the embankment and the results are averaged over three measurements taken at the three locations around the center of measuring stations. SV 6 is the case in which vegetation was not installed, while SV 15 is the case with vegetation mat installed. As can be seen in the figure, the loss rate was significantly reduced when the vegetation was installed.

Fig. 7. Velocity contour and soil loss rate for two experimental cases with and without vegetation (Series SV)

Table 2 summarizes the HV tests. As in the series SV, the protective effect of the vegetation is evident. The cases with vegetation exhibit 21 to 44% less soil loss, demonstrating the protective effect of vegetation. In particular, the average soil loss rate in cases without a vegetation mat (HV 1 to 9) was 37.34%, and that of cases with a vegetation mat (HV 10 to 18) was 6.13%.

One can observe that the greatest loss occurred at a depth of 0.3 m (Table 2, SV9), and the loss rate was 60.9% at a speed of 1.0 m/s. To illustrate the effect of the vegetation, the difference between the HV 3 and HV 12 loss rates was 32.22%; that between HV 6 and HV 15 was 38.82%, and that between HV 9 and HV 18 was 44.95%. In addition, with the same flow rate, the difference in the loss rate depending on the changes of the water depth at the sectional maximum current speed of 1.0 m/s was 25.43% when there was no vegetation mat, and it was 12.73% when there was a vegetation mat, and this difference was lower than when there was no vegetation mat. From the results of the hydraulic experiments conducted to evaluate the safety of the revetment, the highest loss rate was at a height 0.3 m. When the vegetation mat was not installed, significant loss occurred in the upper part of the slope above the water surface. This loss seems to be due to the upper part falling as the lower part of the high water revetment was eroded. Such a phenomenon usually occurs at the time of erosion of a revetment in rivers.

Fig. 8. Velocity contour and soil loss rate for two experimental cases with and without vegetation (Series HV)

4.2 Prototype-scale experiments

Table 8 summarizes the results from the prototype-scale experiments (series PV). Fig. 9 depicts the results for the loss rate in the prototype channel. In series PV, the cross-sectional average flow rate was shown to be in the range of 1.3 m^3/s to 6.5 m^3/s, which are at least an order of magnitude greater than the laboratory-scale experiments. The soil loss rate increases with the flow rate and ranges between 9.8 and 29.55%. The scour patterns occurred mostly in the lower part of the embankment that is in constant contact with the flowing water. Note that area of soil loss grows upward with increasing water depth. This behavior is explained by the fact that the main soil failure mode is sliding, which is usually initiated when the channel bed scours and undermines the toe of the riprap blanket. This could be caused by particle erosion of the toe material, or some other mechanism which causes displacement of toe material (Brown and Clyde, 1989).

Fig. 9. Soil Loss Rate Results (Series PV)

4.3 Soil loss rate as a function of Froude numbers

The experimental results are obtained from a variety of channel cross-section geometries and two widely different scales. To analyze those in a consistent framework, the results are recast in terms of Froude numbers. Two kinds of Froude numbers were introduced in Section 2: Fr_h is based on the nominal water depth h; and Fr_R is based on the hydraulic radius R. Figures 10 and 11 show the soil loss rate (SLR) as a function of Fr_h and Fr_R, respectively, for entire experimental cases.

Fig. 10. Soil loss rate (SLR) as a function of Fr_h.

Fig. 11. Soil loss rate (SLR) as a function of Fr_R.

In both series SV and HV, in which two sets of experiments were carried out with and without vegetation mat, respectively, effectiveness of the vegetation mat in reducing the soil loss rate is apparent. For the series SV, the soil loss rate is reduced by a factor of two when vegetation mat is installed, while it is as large as a factor of six for the series HV. Without the protection by the vegetation mat, the series HV shows much more soil loss rate compared to that of series SV. As mentioned in the previous section, this is because the soil used in the series SV was excavated from a natural river bank, and is more consolidated and resistant to erosion compared to the soil used in the series HV. It is remarkable, however, that the vegetation mat performs so well in the series HV, and the results from both SV and HV could be fitted with one linear line. On the other hand, the soil used in the series PV is the same kind as that of HV, and the result shows that the gradient of the soil loss rate increases with the Froude number, suggesting a power-law relationship.

4.4 Curve fitting

For the experimental cases with the vegetation mat installed, the soil loss rate results are least-squared fitted with power functions of Fr_h (Fig. 12) and Fr_R (Fig. 13), respectively. It is appropriate to only include the results from the series HV and PV in this analysis since the same kind of soil was used for the two series, which is shown in Fig. 12(a) and 13(a). However, observing from Figs. 10 and 11 that the soil loss rate results from both SV and HV seem to fit with a single linear line, it is also tempting to include the results from the series SV, as displayed in Fig 12(b) and 13(b). Fitted power functions are listed in table 4.

Fig. 12(a). Soil loss rate (SLR) as a function Fr_h for the series HV (with mat) and PV.

Fig. 12(b). Soil loss rate (SLR) as a function Fr_h for the series SV (with mat), HV (with mat) and PV.

Fig. 13(a). Soil loss rate (SLR) as a function Fr_R for the series HV (with mat) and PV.

Fig. 13(b). Soil loss rate (SLR) as a function Fr_R for the series SV (with mat), HV (with mat) and PV.

Overall, it seems that the soil loss rate is more or less proportional to the square of Froude number. However, the results from the series HV spread over a relatively wide range, which causes a significant underprediction of the fitted functions for large Froude numbers. This indicates that other flow and channel characteristics, which are not reflected in the definition of the Froude numbers, may play a role, and further study would be needed to elucidate the details.

4.4 The soil loss rate as a function of the cross-sectional average velocity

The purpose of the present study is to provide a practical guideline in designing and installing vegetation mats. In practice, the cross-sectional average velocity (U) is used rather than the Froude number as the design parameter (Busan Regional Construction Management Administration, 2008). Accordingly, the results are replotted as a function of U in Fig. 14. As in Figs. 12 and 13, the results from the series SV as well as HV and PV are included.

Fig. 14(a). Soil loss rate (SLR) as a function U for the series HV (with mat) and PV.

Fig. 14(b). Soil loss rate (SLR) as a function U for the series SV (with mat), HV (with mat) and PV.

Also depicted in the figure are the fitted power functions and table 5 lists the curve-fitting results. Again the spread of the results from the series HV is noted, but the coefficient of the determination (R-square value) is around 0.8, which is encouraging. We emphasize here that this is practically the first guideline for vegetation mat design based on experimental data including the large-scale prototype experiments.

5. Conclusion

In this study, the effects of vegetation on the loss rate of the earthed soil were studied via both laboratory-scale hydraulic experiments and prototype-scale experiments. Overall, experimental results demonstrate that a revetment with vegetation greatly reduces the soil loss rate. To analyze the experimental results obtained from a wide disparity of scales, the results were recast in terms of Froude numbers. While the results from the laboratory-scale experiments suggest a linear relationship between the soil loss rate and the Froude number, we observed that the gradient of soil loss rate rapidly increases as the Froude number approaches 1. The large Froude numbers could only be achieved in the prototype-scale experiments, which highlights the importance of large-scale experiments in establishing design standards for hydraulic structures. To provide a guideline in actual design practices, the soil loss rate as a function of the cross-sectional average velocity has also been provided.

With the increase of the number of river bank naturalization projects using the environmentally friendly vegetation mat method, the methodology and results established in the present study should be useful for predicting the soil loss rate as a function of slope, flow velocity and water depth. This information is especially useful in assessing the stability of the revetment. As a future study, further large-scale experiments that incorporate curved sections of the river and the three-dimensional structure of the revetment would provide useful information.

Acknowledgement

This article was based on numerous research activities conducted in Ecoriver21 (2006, B01), which was supported by Ministry of Land, Infrastructure and Transport of Korean government (MLIT, KAIA).

References

Busan Regional Construction Management Administration, 2008. Stream Revetment Design (Grass line & Vegetation Mat).

Brown, S.A., and Clyde, E.S. 1989. Design of Riprap Revetment, HEC-11, U.S.DOT, FHWA Technical Report, FHWA-IP-89-016.

Järvelä, J., 2004. Determination of flow resistance caused by nonsubmerged woody vegetation. Int. J. River Basin Manage. 2 (1), pp.61–70.

Kouwen, N., Fathi-Moghadam, M., 2000. Friction factors for coniferous trees along rivers. J. Hydraulic Eng. 126 (10), pp.732– 740.

Kouwen, N., Unny, T.E., 1973. Flexible roughness in open channels. J. Hydraulics Div. ASCE 99 (5), pp.713–728.

Lápez, F., and García, M.H., 2001. Mean flow and turbulence structure of open-channel flow through non-emergent vegetation. J. Hydraulic Eng. 127 (5), pp.392–402.

Naot, D., Nezu, I., Nakagawa, H., 1996. Unstable patterns in partly vegetated channels. J. Hydraulic Eng. 122 (11), pp. 671–673.

Nepf, H. M., 1999. Drag turbulence and diffusion in flow through emergent vegetation. Water Resource Research,Vol. 35, No. 2, pp. 479–489.

Shimizu, Y., and Tsujimoto, T., 1994.Numerical analysis of turbulent open-channel flow over a vegetation layer using a k-ε turbulence model. J Hydrosci Hydraulic Eng 11 (2), pp.57–67.

Stephan, U., and Gutknecht, D., 2002. Hydraulic resistance of submerged flexible vegetation. J. Hydrol. 269 (1/2), pp.27–43.

Temple, D. M., 1987. Closure to velocity distribution coefficients for grass-lined channels. Journal of Hydraulic Engineering113 (9), pp.1221–1226.

Table 1. Experimental cases and results (Series SV)

Case	Q (m^3/s)	Revetment Slope	u (m/s)	h (m)	w (m/s)	d (m)	R	Fr_h No	Fr_R No	SLR (%)	Slope condition
SV 1	0.016	1.0	0.20	0.4	0.9	0.31	0.19	0.11	0.15	3.48	Silt
SV 2	0.040	1.0	0.51	0.4	0.9	0.31	0.19	0.29	0.37	6.68	Silt
SV 3	0.064	1.0	0.80	0.4	0.9	0.31	0.19	0.46	0.58	7.28	Silt
SV 4	0.024	1.5	0.22	0.4	0.9	0.27	0.17	0.13	0.17	3.09	Silt
SV 5	0.060	1.5	0.53	0.4	0.9	0.27	0.17	0.33	0.41	7.75	Silt
SV 6	0.096	1.5	0.82	0.4	0.9	0.27	0.17	0.51	0.64	9.20	Silt
SV 7	0.032	2.0	0.23	0.4	0.9	0.22	0.14	0.16	0.19	4.13	Silt
SV 8	0.080	2.0	0.52	0.4	0.9	0.22	0.14	0.35	0.44	11.79	Silt
SV 9	0.128	2.0	0.84	0.4	0.9	0.22	0.14	0.57	0.71	17.22	Silt
SV 10	0.016	1.0	0.19	0.4	0.9	0.31	0.19	0.11	0.14	0.08	Vegetation
SV 11	0.040	1.0	0.50	0.4	0.9	0.31	0.19	0.29	0.37	2.24	Vegetation
SV 12	0.064	1.0	0.79	0.4	0.9	0.31	0.19	0.45	0.58	4.66	Vegetation
SV 13	0.024	1.5	0.18	0.4	0.9	0.27	0.17	0.11	0.14	0.30	Vegetation
SV 14	0.060	1.5	0.51	0.4	0.9	0.27	0.17	0.31	0.40	1.74	Vegetation
SV 15	0.096	1.5	0.79	0.4	0.9	0.27	0.17	0.49	0.61	5.09	Vegetation
SV 16	0.032	2.0	0.20	0.4	0.9	0.22	0.14	0.14	0.17	1.61	Vegetation
SV 17	0.080	2.0	0.51	0.4	0.9	0.22	0.14	0.35	0.43	4.13	Vegetation
SV 18	0.128	2.0	0.78	0.4	0.9	0.22	0.14	0.53	0.66	5.65	Vegetation

Table 2. Experimental cases and results (Series HV)

Case	Q (m^3/s)	Revetment Slope	u (m/s)	h (m)	w (m/s)	d (m)	R	Fr_h No	Fr_R No	SLR (%)	Slope condition
HV 1	0.018	1.5	0.56	0.20	0.60	0.15	0.10	0.46	0.55	23.29	Sand
HV 2	0.024	1.5	0.76	0.20	0.60	0.15	0.10	0.63	0.75	27.02	Sand
HV 3	0.030	1.5	0.99	0.20	0.60	0.15	0.10	0.82	0.98	35.47	Sand
HV 4	0.028	1.5	0.60	0.25	0.68	0.18	0.12	0.45	0.55	34.46	Sand
HV 5	0.038	1.5	0.80	0.25	0.68	0.18	0.12	0.60	0.73	39.99	Sand
HV 6	0.047	1.5	0.98	0.25	0.68	0.18	0.12	0.74	0.90	44.25	Sand
HV 7	0.041	1.5	0.60	0.30	0.75	0.21	0.14	0.42	0.52	30.64	Sand
HV 8	0.054	1.5	0.83	0.30	0.75	0.21	0.14	0.58	0.71	40.01	Sand
HV 9	0.068	1.5	0.99	0.30	0.75	0.21	0.14	0.69	0.85	60.90	Sand
HV 10	0.018	1.5	0.55	0.20	0.60	0.15	0.10	0.45	0.54	2.23	Vegetation Mat
HV 11	0.024	1.5	0.73	0.20	0.60	0.15	0.10	0.60	0.72	3.14	Vegetation Mat
HV 12	0.030	1.5	0.93	0.20	0.60	0.15	0.10	0.77	0.92	3.52	Vegetation Mat
HV 13	0.028	1.5	0.59	0.25	0.68	0.18	0.12	0.44	0.54	3.53	Vegetation Mat
HV 14	0.038	1.5	0.80	0.25	0.68	0.18	0.12	0.60	0.73	4.58	Vegetation Mat
HV 15	0.047	1.5	0.98	0.25	0.68	0.18	0.12	0.74	0.90	5.43	Vegetation Mat
HV 16	0.041	1.5	0.60	0.30	0.75	0.21	0.14	0.42	0.52	6.11	Vegetation Mat
HV 17	0.054	1.5	0.82	0.30	0.75	0.21	0.14	0.57	0.70	10.39	Vegetation Mat
HV 18	0.068	1.5	0.97	0.30	0.75	0.21	0.14	0.68	0.83	16.25	Vegetation Mat

Table 3. Experimental cases and results (Series PV)

Case	Q (m^3/s)	Revetment Slope	u (m/s)	h (m)	w (m/s)	d (m)	R	Fr_h No	Fr_R No	SLR (%)	Slope condition
PV 1	1.16	2.0	1.18	0.27	4.18	0.24	0.23	0.78	0.79	9.80	Vegetation Mat
PV 2	2.18	2.0	1.49	0.38	4.62	0.32	0.31	0.84	0.86	17.00	Vegetation Mat
PV 3	3.15	2.0	1.70	0.46	4.94	0.37	0.36	0.89	0.91	20.60	Vegetation Mat
PV 4	4.01	2.0	1.86	0.52	5.18	0.42	0.40	0.92	0.94	27.80	Vegetation Mat
PV 5	4.93	2.0	1.99	0.58	5.42	0.46	0.43	0.94	0.97	29.55	Vegetation Mat

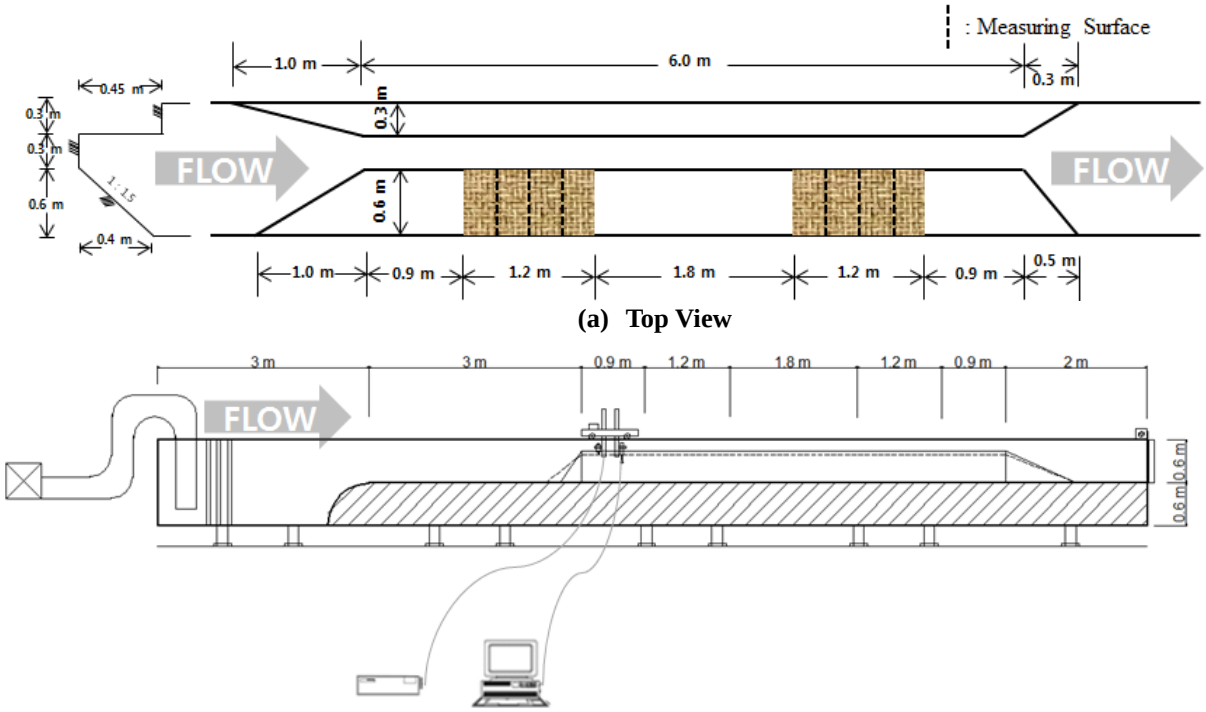

(a) Top View

(b) Side View

Fig. 1. Schematic diagram of the experimental channel.

Fig. 2. Acrylic embankment and vegetation mat installed in the channel

Fig. 3 Vegetation and vegetation mat installed in the channel

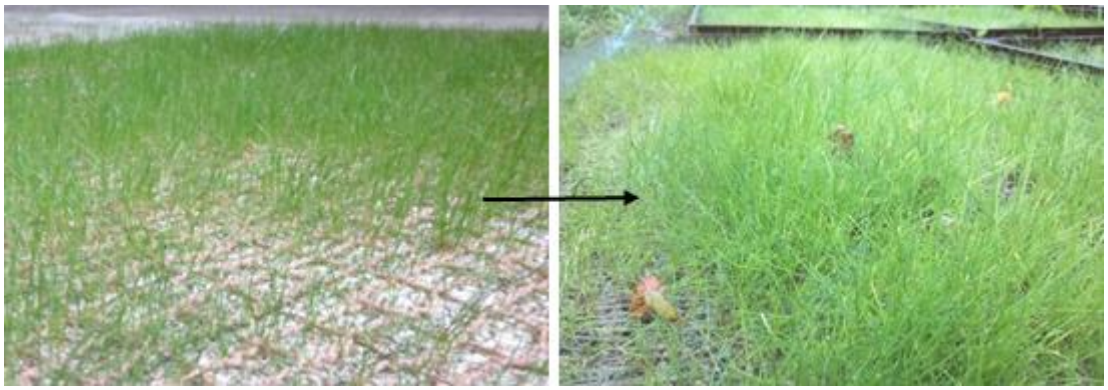

Fig. 4 Vegetation mat growing processes (after 2weeks and 4weeks, respectively)

Fig. 5. Multi-functional river experiment station in Korea

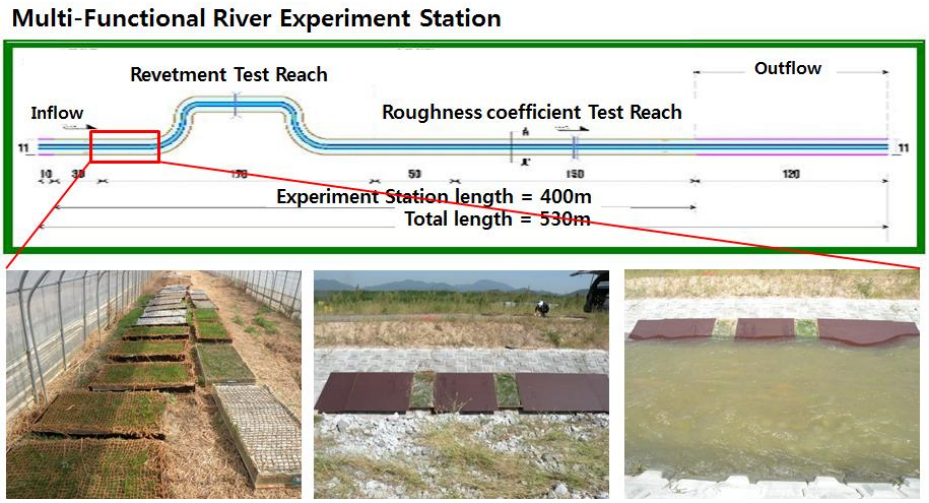

Fig. 6. Vegetation mats installed in the experimental channel

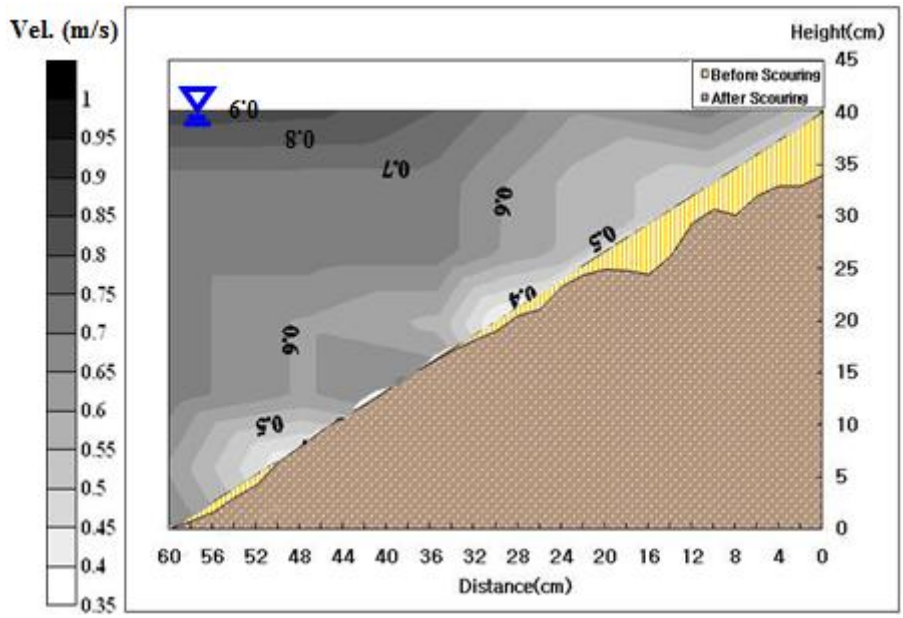

(a) SV 6 Results

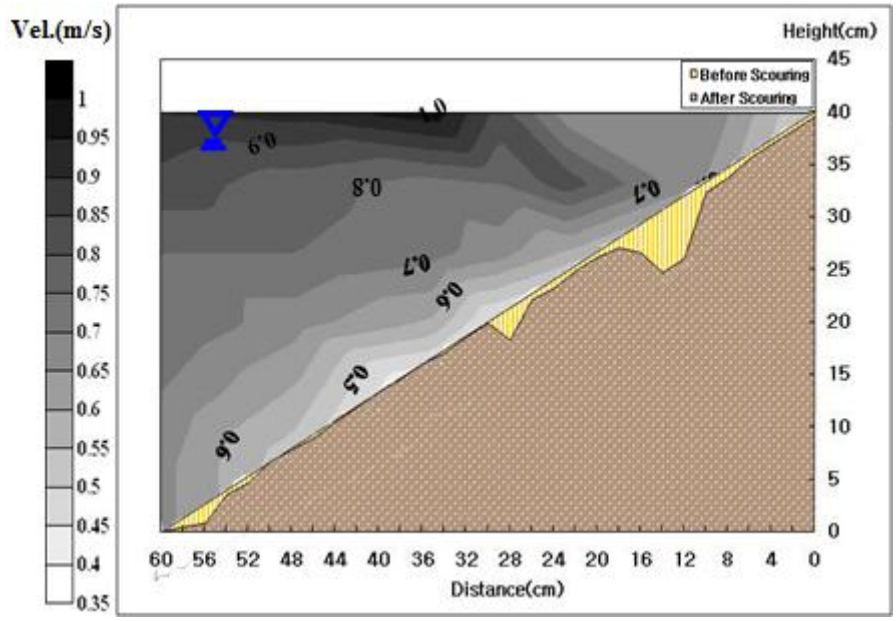

(b) SV 15 Results

Fig. 7. Velocity contour and soil loss rate for two experimental cases with and without vegetation (Series SV)

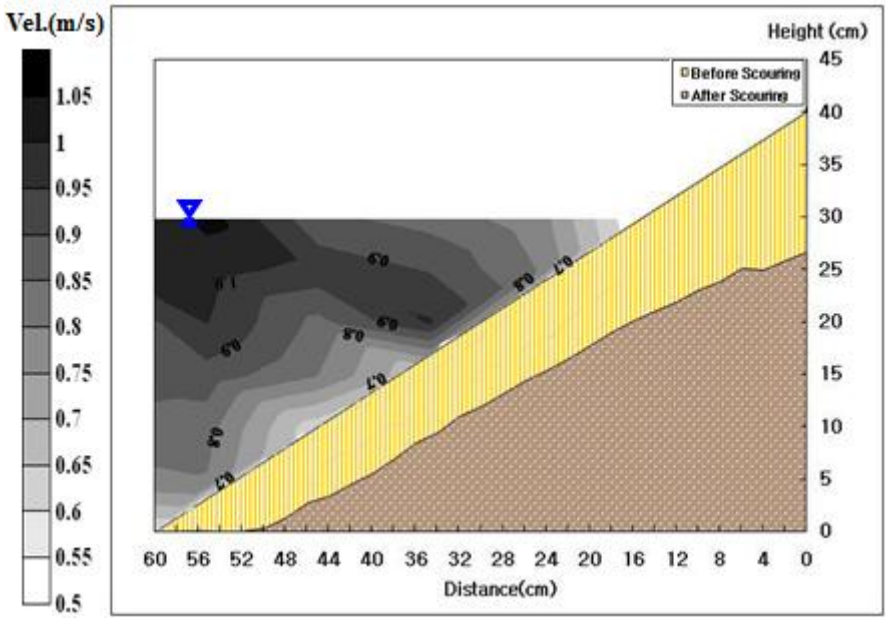

(a) HV 6 Results

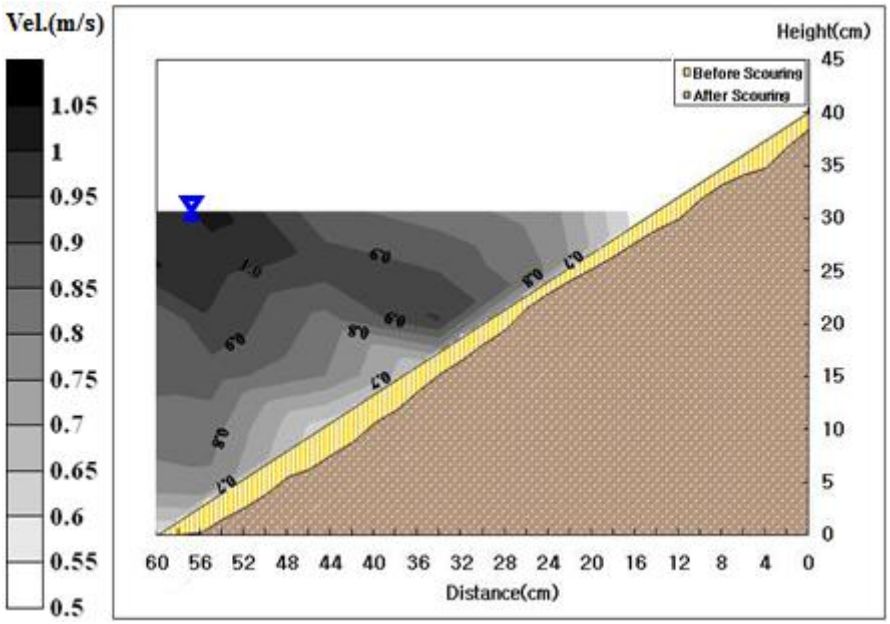

(b) HV 15 Results

Fig. 8. Velocity contour and soil loss rate for two experimental cases with and without vegetation (Series HV)

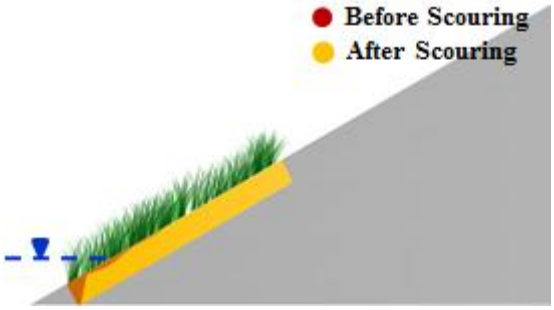

(a) PV1 Results

(b) PV2 Results

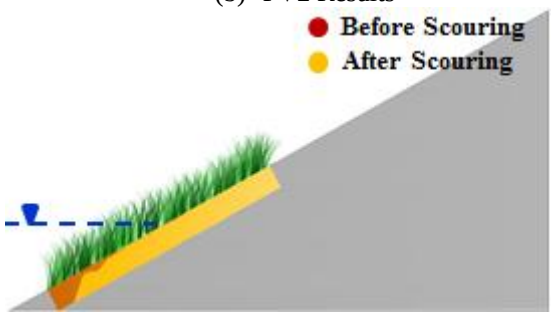

(c) PV3 Results

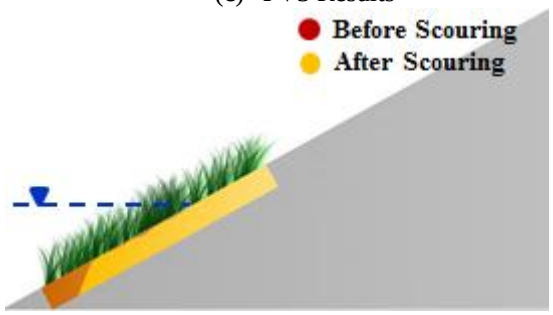

(d) PV4 Results

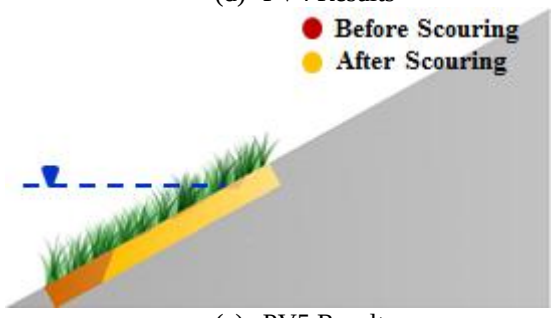

(e) PV5 Results

Fig. 9. Soil Loss Rate Results (Series PV)

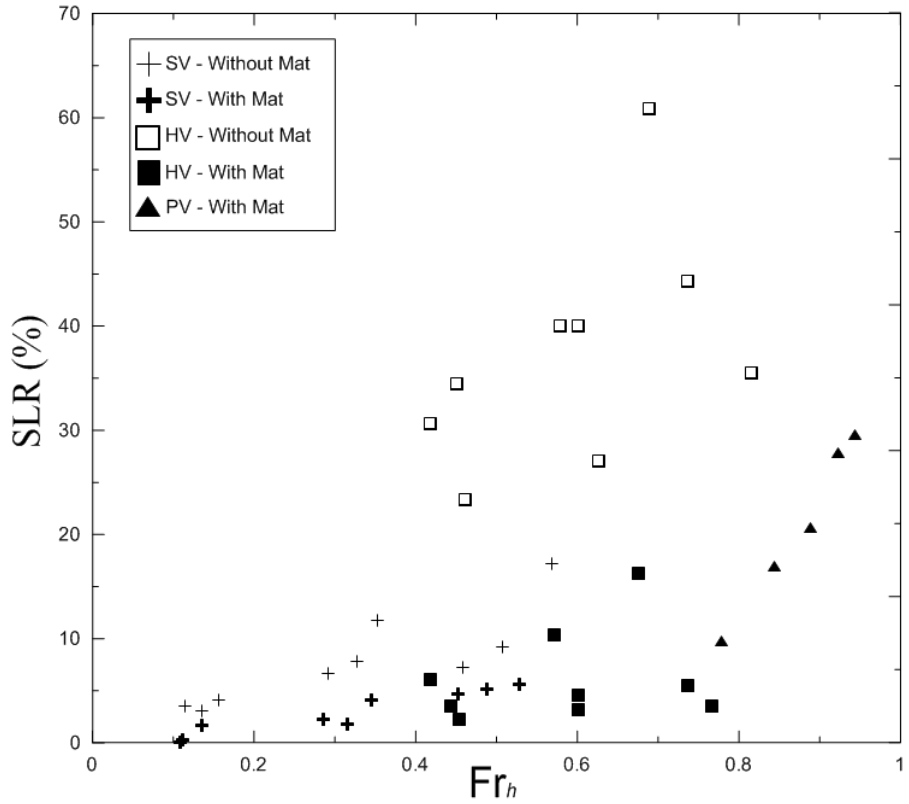

Fig. 10. Soil loss rate (SLR) as a function of Fr_h.

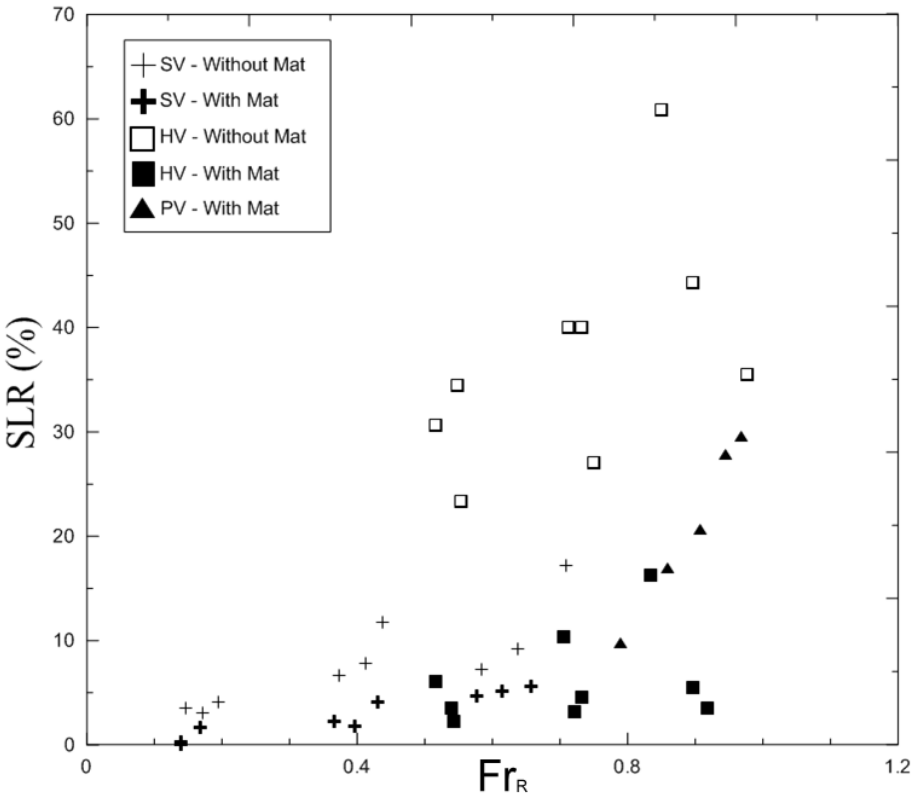

Fig. 11. Soil loss rate (SLR) as a function of Fr_R.

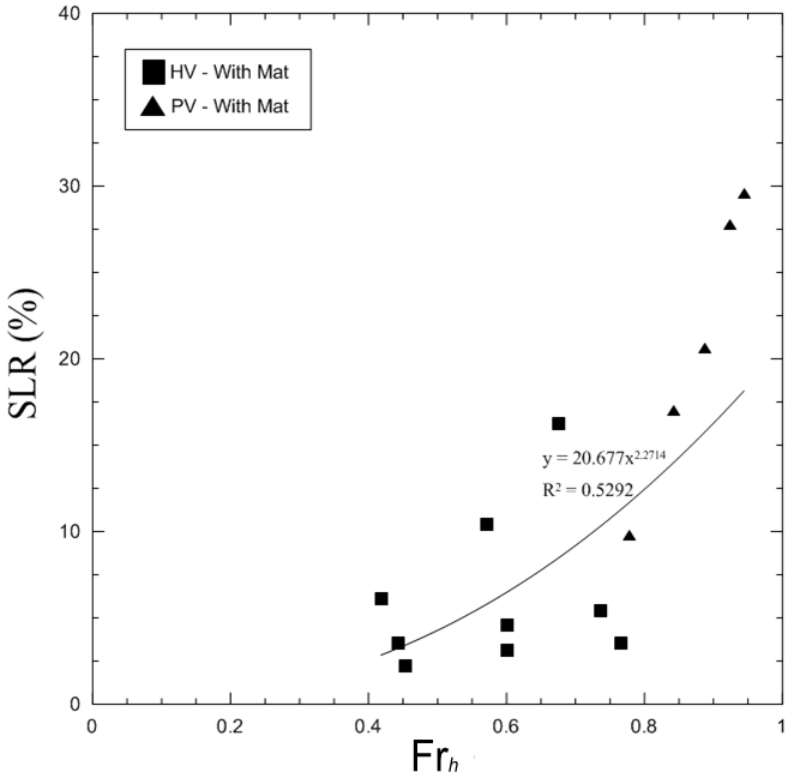

Fig. 12(a). Soil loss rate (SLR) as a function Fr_h for the series HV (with mat) and PV.

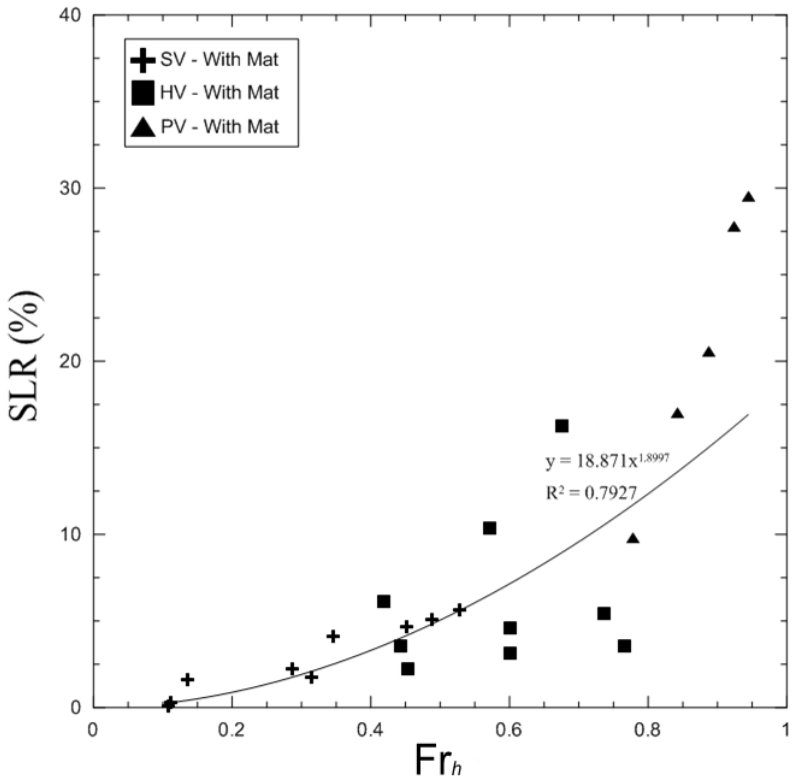

Fig. 12(b). Soil loss rate (SLR) as a function Fr_h for the series SV (with mat), HV (with mat) and PV

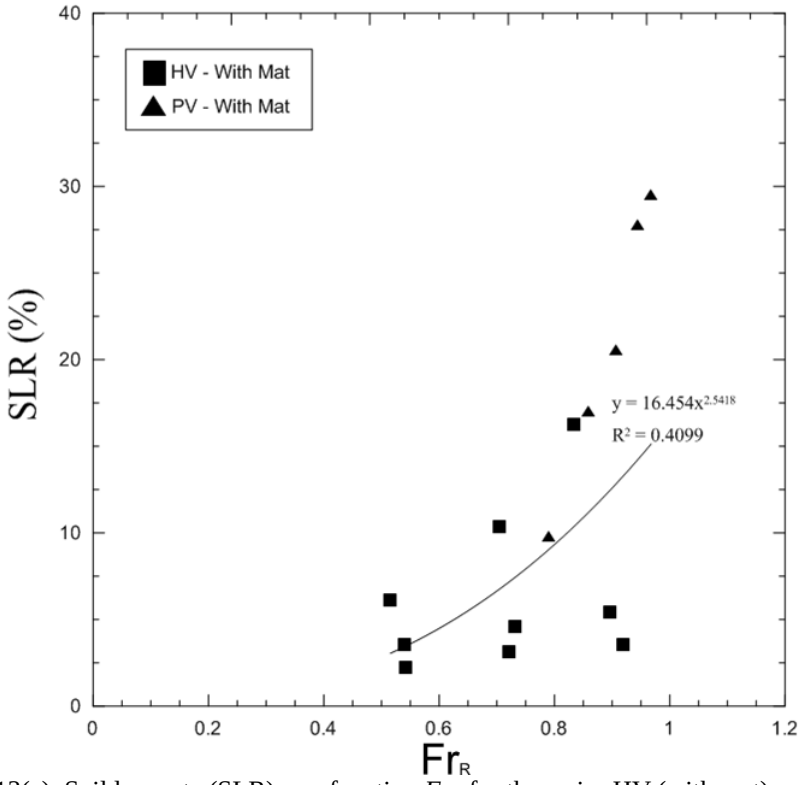

Fig. 13(a). Soil loss rate (SLR) as a function Fr_R for the series HV (with mat) and PV.

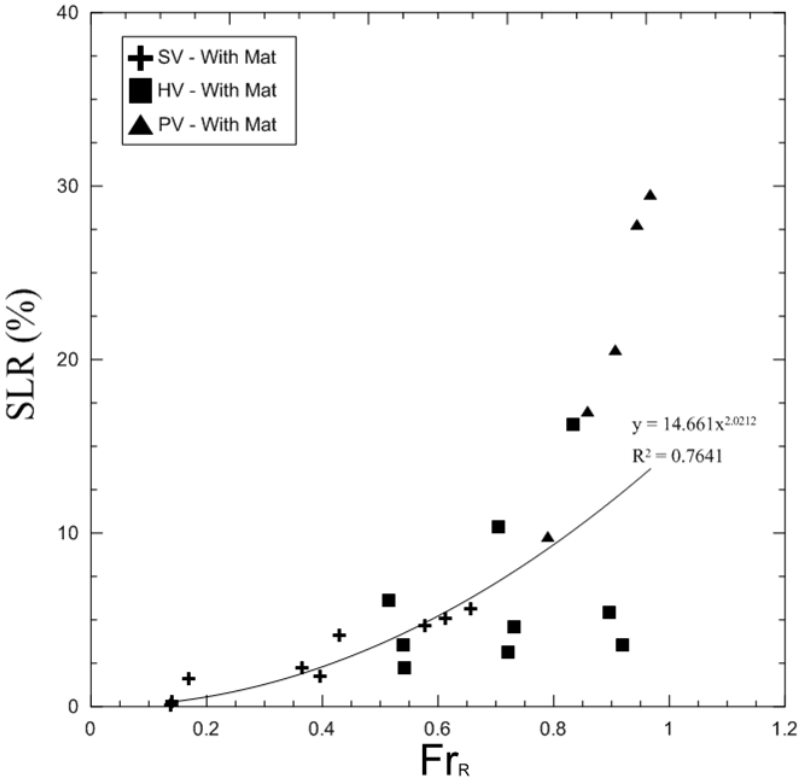

Fig. 13(b). Soil loss rate (SLR) as a function Fr_R for the series SV (with mat), HV (with mat) and PV.

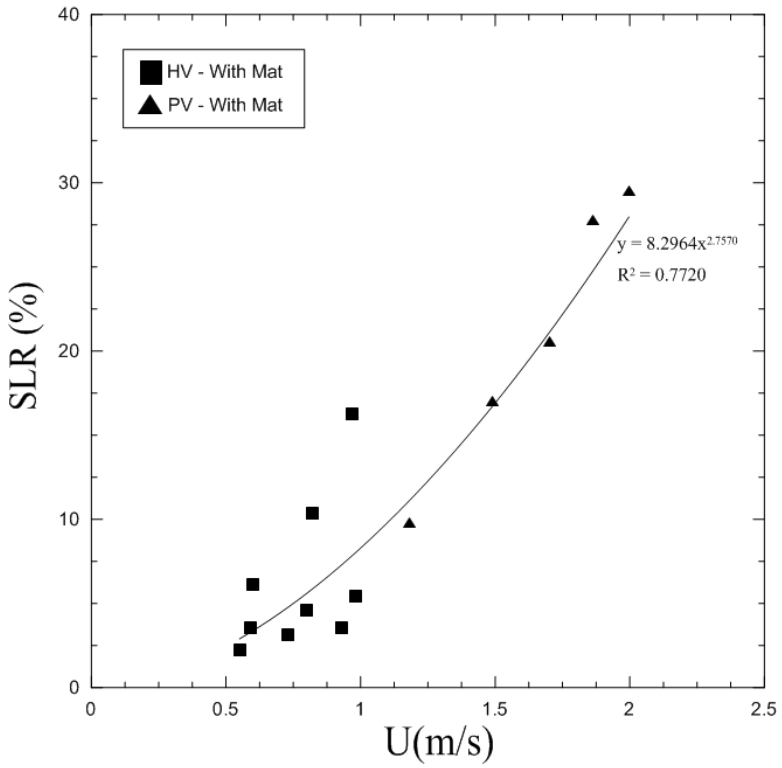

Fig. 14(a). Soil loss rate (SLR) as a function *U* for the series HV (with mat) and PV.

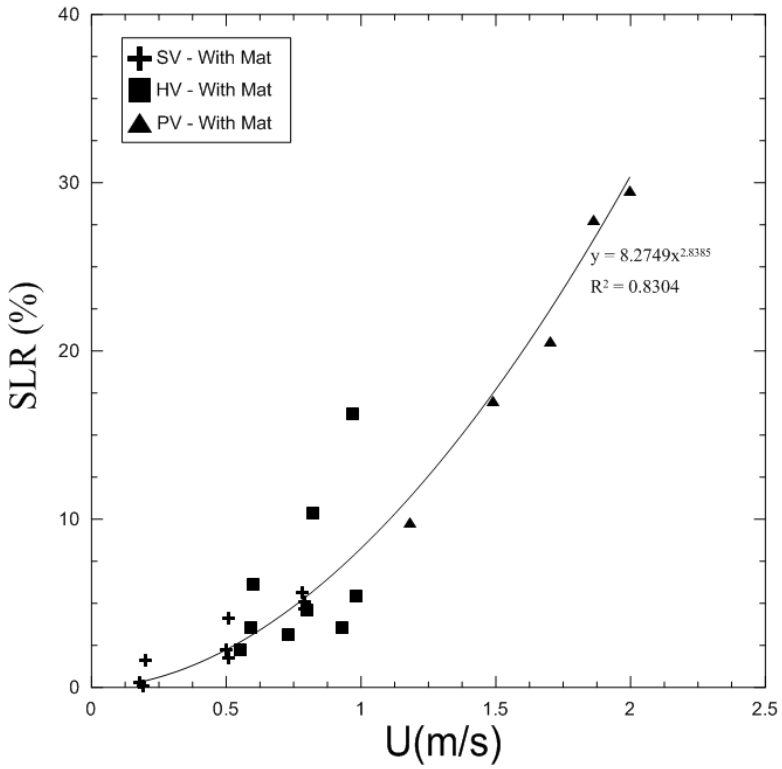

Fig. 14(b). Soil loss rate (SLR) as a function *U* for the series SV (with mat), HV (with mat) and PV.